

Particle Exhaust and Scrape-Off Layer Conditions in ELM Suppressed Resonant Magnetic Perturbation Discharges on DIII-D

E.A. Unterberg¹, J.M. Canik², T.E. Evans³, R. Maingi², O. Schmitz⁴, N.H. Brooks³,
M.E. Fenstermacher⁵, R.A. Moyer⁶, and J.G. Watkins⁷

¹Oak Ridge Institute for Science Education, Oak Ridge, Tennessee, USA

²Oak Ridge National Laboratory, Oak Ridge, Tennessee, USA

³General Atomics, PO Box 85608, San Diego, California 92186-5608, USA

⁴Forschungszentrum-Jülich, Jülich, Germany

⁵Lawrence Livermore National Laboratory, Livermore, California, USA

⁶University of California-San Diego, La Jolla, California, USA

⁷Sandia National Laboratories, Albuquerque, New Mexico, USA

The complete suppression of edge localized modes (ELMs) in a tokamak using the resonant component of a 3D magnetic perturbing field (RMP) has been demonstrated on DIII-D at ITER similar pedestal electron collisionalities and cross-sectional shapes [1]. Accompanying the suppression is an increase in particle transport leading to the reduction in density across the entire minor radius. It is observed that the pedestal density reduction varies from 2%–30% of the ELMy H-mode density but shows no obvious correlation with the magnitude of perturbing coil current [2,3]. Further investigations of the particle sources and sinks identified a bifurcation in edge plasma conditions and divertor pumping characteristics when the divertor magnetic topology is varied [4]. Figure 1 shows how the divertor has been modified in the lower divertor pump-baffling with the configuration in Fig. 1(a) termed “ITER similar shaped (ISS)” ($\langle\delta\rangle \sim 0.5$) and that in (b) termed “Low- $\langle\delta\rangle$ ” (~ 0.3). As shown in Fig. 1(c), the total pressure in the plenums is roughly the same, at ~ 0.35 mTorr, before the RMP is applied. The pressure then drops to near zero in the Low- $\langle\delta\rangle$ configuration while slightly increasing and remaining at ~ 0.45 mTorr in the ISS configuration after the RMP application. Field line tracing identified changes to the divertor magnetic topology due to the perturbed separatrix in the two configurations. Here we investigate why the plenum pressure

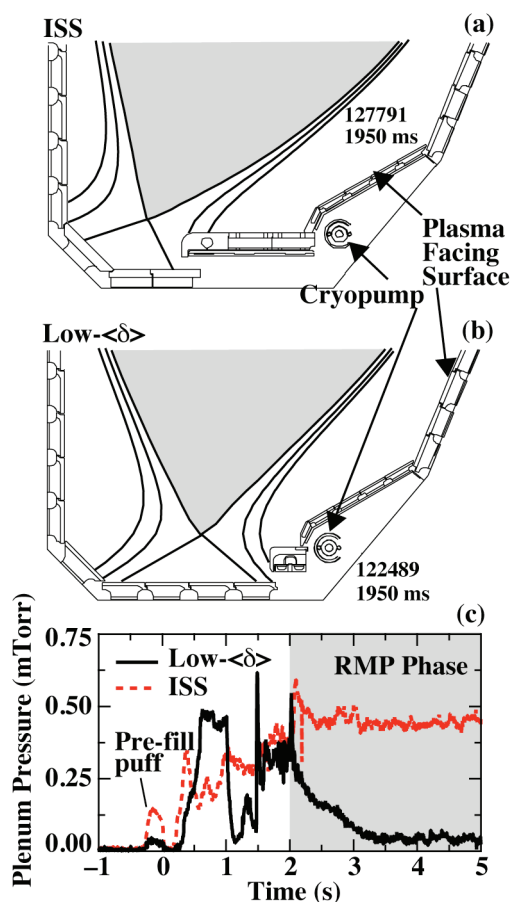


Fig. 1. Poloidal view of the lower divertor region showing the (a) extended baffling modification compared to (b) the original baffling. (c) Shows the difference in pumping between the two configurations.

remains high in the ISS configuration, which in turn gives simultaneous ELM suppression and particle exhaust control.

Recent analysis suggests that the perturbed equilibrium causes short connection length field lines to intersect the first wall which lead to an increase in particle transport to the newly wetted surfaces [6,7]. Figure 2 shows the calculated field-line loss pattern at the first wall for both configurations shown in Fig. 1(a) and 1(b) using the TRIP3D vacuum field line following code [8]. The set of edge diagnostics used in the SOLPS modeling is overlaid to show how the 3D structure potentially intersects local diagnostic views. The ISP and OSP is seen quite clearly in each sub-figure at $\theta \sim (-115^\circ)$ and $\sim (-100^\circ)$, respectively. The splitting of the strikepoints due to the RMP is also obvious. The most striking difference between the two configurations is the larger splitting of the strikepoints in the ISS case [Fig. 2(b)]. Here it can be seen in the ISS case [Fig. 3(b)] that the perturbed separatrix envelops the outer target and lower shelf [$\theta \sim (-80^\circ)$ through (-120°)]. On the other hand, Fig. 2(a) shows the splitting to be reduced, with only a few striations leaving the lower divertor region at $\phi \sim 270^\circ-360^\circ$. It is thought that the coupling of this increased splitting with the outer pump plenum is the cause of the increase neutral exhaust seen in Fig. 1(c). Therefore the ISS configuration is the focus of more detailed study.

The principle diagnostics of this study include line-emission spectroscopy arrays of which there is an

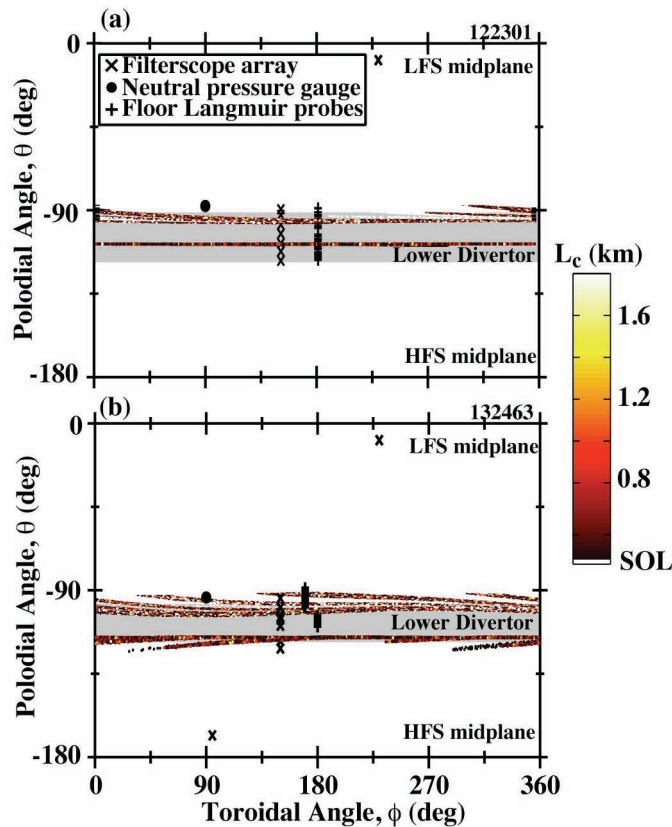


Fig. 2. Comparison of the perturbed field-line pattern (via L_c) to the first wall of DIII-D with an overlay of relevant wall diagnostics between the two configurations. (a) is of the low-d configuration and (b) is of the ISS configuration. The lower divertor target region is highlighted in grey.

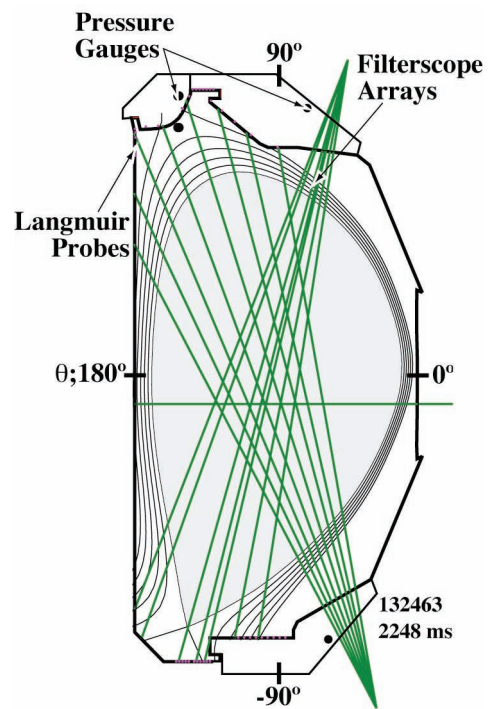


Fig. 3. Poloidal view of edge diagnostics.

extensive poloidal array (Fig. 3) with a minimal toroidal coverage (Fig. 2). There are also four fast neutral pressure gauges located in both the upper and lower divertor cryopump plenum regions as well as one in upper dome region of vessel (Fig. 3). Langmuir probes are embedded into the graphite tiles in both the upper and lower divertor regions [5]. Finally, midplane profiles of plasma parameters are taken from fits to Thomson scattering data and from a tangential midplane line emission spectrometer system. These two systems give the upstream profiles of n_e , T_e , and D_α emissivity which are then used constrain edge modeling with SOLPS. The discharge is termed an ISS discharge because it has an averaged triangularity, $\langle \delta \rangle$, ~ 0.5 and pedestal collisionality similar to those expected in ITER ($\nu_e^* \sim 0.1$) [1]. In particular, it has the following parameters during the RMP phase; $I_p = 1.57$ MA, edge electron collisionality, $\nu_e^* = 0.07\text{--}0.11$, $q_{95} = 3.49$, $P_{\text{NBI}} = 7.85$ MW, $n_e/n_{\text{GW}} = 0.29$, and $\beta_N = 1.6\text{--}2.4$, which are typical parameters for RMP ELM suppression studies in ISS discharges on DIII-D [1,9].

An increase in edge particle flux to the walls [4–6] and an increase in particle exhaust to the cryopumps is observed with RMP application, as shown in Fig. 1(c). This is correlated to the increase in D_α signal from filterscope arrays [3,4] and ion saturation current from Langmuir probes [5], and is further correlated with a redistribution of short connection length field lines due to the RMP [6]. Although the vacuum modeling of the field lines suggest the perturbed field is confined to the lower divertor region (Fig. 3), diagnostics in the upper divertor, specifically, indicate increased particle flux in this region as well. Figure 4 shows the pump plenum pressure from fast ionization gauges in both the upper and lower divertor (Fig. 2). Here it is seen that most of the exhaust pressure in an ISS discharge occurs in the lower pump plenum, as expected for a LSN discharge. However, upon application of the RMP the signal on the gauges in the upper divertor respond and evolve in time as the RMP phase progresses. This suggests an initial flux of neutrals to this region, followed by a slow buildup of these neutral particles. This observation of slowly increasing neutral pressure is corroborated by calculating the percent change in the D_α signal in the upper divertor, which also show an increasing D_α signal during the application of the RMP [Fig. 5(c) and 5(d)]. The D_α signal from the lower divertor outer strikepoint is shown in Fig. 5(a) as a baseline reference signal. Figure 5(b–d) then shows the change relative to this baseline signal for chords viewing the lower shelf, upper shelf, and

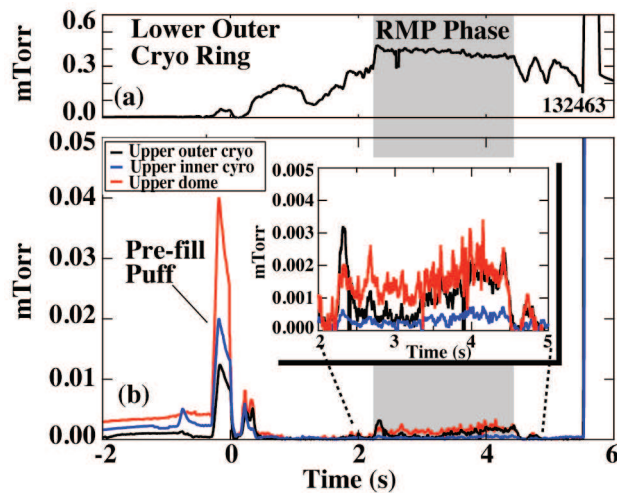


Fig. 4. Neutral pressure measurements in (a) the lower pump plenum and (b) the upper divertor region.

upper dome region, respectively. Here a slow increase in the signal is seen with a time delay in the response between the three viewchords moving from the lower shelf to the upper dome, Fig. 5(b–d). The most striking point of this observation is the time delay as the poloidal angle increases from $\theta \sim -90^\circ$ to 90° (i.e., going from the lower shelf to the upper divertor region). One explanation for the delay is that the perturbed separatrix is now heating the lower shelf where a linear increase in D_α intensity throughout the RMP phase is observed [Fig. 5(b)]. This linear rise in signal is thought to be due to the heating that is then slowly liberating neutrals from the shelf. The time delay of ~ 1 s between the chords is still a mystery. Further modeling with SOLPS is anticipated to provide a better understanding of this mystery.

In summary, differences in the particle exhaust during RMP ELM suppressed discharges with different divertor configurations are observed. This difference is attributed to changes in the divertor magnetic topology due to the RMP field. Observations of neutral pressure and D_α suggest there is increased particle transport outside the lower divertor region (for a LSN discharge). These observations couple with an increase in particle exhaust that enhances the capture of efflux particles during the RMP and gives both ELM suppression and particle exhaust control in ISS discharges on DIII-D. Although a complete understanding is still missing, the importance of the 3D magnetic topology not only for the suppression of ELMs but also for particle control is an important area of investigation for next step devices.

This work was supported in part by the US Department of Energy under DE-AC05-06OR23100, DE-FC02-04ER54698, DE-AC05-00OR22725, and DE-AC52-07NA27344.

References

1. T.E. Evans, *et al.*, Nucl. Fusion **48** (2008) 024002.
2. E.A. Unterberg, *et al.*, J. Nucl. Mater. **390-391** (2009) 486.
3. E.A. Unterberg, *et al.*, submitted to Nucl. Fusion Lett. (2009).
4. E.A. Unterberg, *et al.*, submitted to Nucl. Fusion (2009).
5. J.G. Watkins, *et al.*, J. Nucl. Mater. **390-391** (2009) 839.
6. O. Schmitz, *et al.*, Plasma Phys. Control. Fusion **50** (2008) 124029.
7. A. Wingen, *et al.*, Phys. Plasmas **16** (2009) 042504.
8. T.E. Evans, *et al.*, Phys. Plasmas **9** (2002) 4957.
9. M.E. Fenstermacher, *et al.*, J. Nucl. Mater. **390-391** (2009) 793.

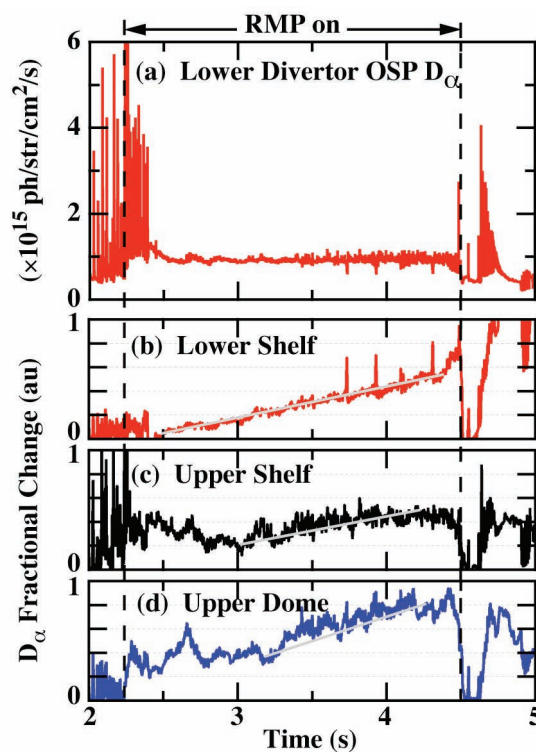


Fig. 5. D_α intensity at the OSP (a) and the change in this OSP D_α relative to other viewchords (b–d).